

# Hybrid quantum-classical computation for automatic guided vehicles scheduling.

Tomasz Śmierzchalski<sup>a</sup>, Łukasz Paweła<sup>a</sup>, Zbigniew Puchała<sup>a</sup>, Mátyás Koniorczyk<sup>b</sup>,  
Bartłomiej Gardas<sup>a</sup>, Sebastian Deffner<sup>c,d</sup>, and Krzysztof Domino<sup>a,\*</sup>

<sup>a</sup>Institute of Theoretical and Applied Informatics, Polish Academy of Sciences, Bałtycka 5, Gliwice, 44-100, Poland

<sup>b</sup>HUN-REN Wigner Research Centre for Physics, Konkoly-Thege Miklós út 29-33., Budapest, 1121, Hungary

<sup>c</sup>Department of Physics, University of Maryland, Baltimore County, Baltimore, Maryland 21250, USA

<sup>d</sup>National Quantum Laboratory, College Park, MD 20740, USA

\*kdomino@iitis.pl

## ABSTRACT

Motivated by global efforts to develop quantum computing for practical, industrial-scale challenges, we showcase the effectiveness of state-of-the-art hybrid quantum-classical solvers in addressing the business-centric optimization problem of scheduling Automatic Guided Vehicles (AGVs). These solvers leverage a noisy intermediate-scale quantum (NISQ) device, specifically a D-Wave quantum annealer. In our study, the hybrid solvers exhibit non-zero quantum processing times, indicating a significant contribution of the quantum component to solution efficiency. This hybrid methodology performs comparably to existing classical solvers, thus indicating ‘quantum readiness’ for scheduling tasks. Our analysis focuses on a practical, business-oriented scenario: scheduling AGVs within a factory constrained by limited space, simulating a realistic production setting. Our new approach concerns mapping a realistic AGV problem onto a problem reminiscent of railway scheduling and demonstrating that the AGV problem more suits quantum computing than the railway counterpart and is more dense in terms of an average number of constraints per variable. We demonstrate that a scenario involving 15 AGVs, which holds practical significance due to common bottlenecks like shared main lanes leading to frequent deadlocks, can be efficiently addressed by a hybrid quantum-classical solver within seconds. Consequently, our research paves the way for the near-future business adoption of hybrid quantum-classical solutions for AGV scheduling, anticipating that forthcoming improvements in manufacturing efficiency will increase both the number of AGVs deployed and the premium on factory space.

## 1 Introduction

Quantum computing, a relatively young science field, has developed rapidly over recent years. It is commonly accepted that this novel technology could shape the future. Certain tasks are not tractable with a classical computer; quantum computing approaches are good candidates to handle these. Algorithms such as Shor’s algorithm<sup>1</sup> proposed a polynomial-time quantum algorithm for the integer factoring problem. At its current development level the improved efficiency offered by quantum computing is restricted to certain computational problems<sup>2</sup>. Nevertheless, it is widely recognized that we are in the era of noisy intermediate-scale quantum (NISQ) devices<sup>3,4</sup>: a few hundred quantum bits are technologically available, but noise and imperfections still have a relevant impact on their operation. Despite that, the first examples of *quantum advantage* have already been presented<sup>5</sup>, and there is an increasing research interest in potential industrial applications that are considered<sup>6–8</sup>. Currently, the community of quantum computing scientists is searching for practical industrial-scale use cases of industrial problems that can be successfully solved using the available quantum devices<sup>9</sup>. Our intention is to address this quest by tackling the Automated Guided Vehicles (AGV) scheduling problem. The size and characteristics of the scheduling problem addressed in this paper make it a good candidate to explore noisy-intermediate scale quantum (NISQ)<sup>3</sup> technologies in industrial applications.

As current quantum devices are small and noisy, hybrid quantum-classical solvers are being developed to handle optimization problems of sizes that are relevant from the practical application point of view. In these hybrid solvers, a part of the computation is performed on a quantum device: the quantum processing unit (QPU), while the so-called master problem is handled by the CPU (central processing unit). Examples of such an approach are the hybrid solvers developed by the D-Wave company<sup>10</sup>. In the present paper, we compare the performance of one of these solvers with a state-of-the-art (classical) integer linear programming (ILP) solver when applied for the scheduling of AGVs. Our findings indicate that in the context of this application, the chosen hybrid solver is comparable with and has the potential to outperform the classical one.

In the broad picture of production scheduling, an approach considered as promising is *Smart Scheduling*<sup>11</sup>. It combines the cyber-physical production systems (CPPS) with the decision support system (DSS). The AGV scheduling optimization can be

treated either as part of the larger industrial system in light of the philosophy of industry 4.0<sup>12</sup> (e.g. together with industrial job scheduling) or just as a sole component. For the sake of demonstration, we focus on the latter. However, our model can be re-integrated into a general DSS system.

Many industrial processes can be optimized, including the design of manufacturing systems and processes, assembly line processes, etc. Within these, we address AGV scheduling, in particular, timetabling in a short time horizon. The decisions have to be made almost in real-time, requiring fast computational heuristics. The concept of industry 4.0<sup>13</sup> implies that AGV scheduling must be tied to the particular factory specifics. To tie our research directly to current business needs, we address a problem that arises in a production environment, i.e. the practice of an actual operating factory. (Its identity and further details are confidential.) We model this particular environment, its configuration, and requirements, addressing the particular needs of the given factory. In this factory, there is a well-defined space where AGVs can maneuver. They are restricted to moving on dedicated "roads" (uni- or bidirectional) to reach ports, loading places, charging stations, etc. Here, the AGVs are controlled by a central system where their scheduling occurs.

AGV scheduling algorithms are divided into rostering<sup>1</sup> and routing<sup>14,15</sup>. The aim of rostering is to dispatch a set of AGVs to perform certain jobs of equipment transportation within the factory. Then, routing (path planning) aims at finding suitable paths for the AGVs, together with the "timetable" and a possible ordering of AGVs passing certain congested places. These problems are commonly solved via linear programming optimization<sup>15,16</sup>.

The work of Tuan<sup>17</sup> provides a fair overview of the optimization of AGVs scheduling. Vehicle rostering is discussed both as an offline scheduling problem (where all transportation requests are known in advance) or as online scheduling (where environments are stochastic, and requirements appear on the fly, c.f. the work of<sup>18</sup>). We follow the approach of deterministic offline scheduling, but each time the circumstances change, we recalculate schedules. An important constraint (tied to time constraints in scheduling theory) is the maximal window of time in which a task has to be performed by an AGV. The objective is a linear function of variables reflecting completion time costs. To solve both static and dynamic problems, most authors apply ILP together with a (custom) column generation approach and various methods of optimization. As we consider routes and tasks of AGVs predefined for our optimization problem, column generation is not applicable.

The literature on bigger-scale AGV scheduling problems is still scarce, and the considered sizes are rather limited when compared to industry practice. For instance, in a recent paper<sup>19</sup>, a system with 9 AGVs is already considered as a large-scale one. In our use case, we introduce a model tailored to the specific needs of this operational setting, employing proprietary hybrid quantum-classical solvers for resolution. In particular, we concentrate on certain components of AGVs scheduling, AGVs' timing, and ordering, stressing the problem of deadlock resolution.

When compared to the most similar contributions in the literature, our approach is complementary to the work of Geitz et al.<sup>8</sup>, where the job scheduling in a factory is optimized on a quantum annealer or classical device. There, however, the focus is on the factory machines. As opposed to that, we focus on the AGV traffic, assuming job assignments to industrial machines are fixed. Haba et al.<sup>20</sup> also addressed a problem of AGV scheduling with quantum methods. There, however, quantum annealing was applied for the routing of AGVs, as opposed to our problem, which addresses the timing and ordering of the AGVs.

The planning of AGVs' paths and task assignment, which is widely analyzed along with scheduling in literature<sup>14</sup>, is not part of our optimization task. We are required to address AGV scheduling in itself, which has less coverage in the literature. Our contribution is the first one in this research direction, which is dedicated to the particular business-driven problem of AGVs scheduling in a factory with limited space.

This particular optimization problem appears to be complex but still tractable for the meaningful number of AGVs (15 AGVs in particular). The anticipated evolution of Industry 4.0, particularly with respect to AGV scheduling, is expected to involve more complex scenarios, such as managing 40 or more AGVs within the confined spaces of a factory. Addressing such challenges in a timely manner could become problematic using common heuristics. Hence, new heuristics or computational paradigms may be necessary for such future applications.

This paper is organized as follows. In Section 3.2, we define our problem and formulate it mathematically. In Section 4, we discuss computational results. In Section 5, we draw conclusions, while Appendix A is devoted to technical details of the mathematical model, and Appendix B is devoted to details on the particular problem of AGVs' scheduling.

## 2 Quantum annealing

A recent theoretical study<sup>21</sup> points toward possible speedup for approximately solving instances of NP-hard combinatorial optimization problems as long as they are implemented using a fault-tolerant quantum computer. Inspired by this, we hope that a quantum-ready model can potentially scale better than classical computer algorithms. Hence, developing quantum hardware may open the possibility of efficiently dealing with large problem instances.

---

<sup>1</sup>also termed as "scheduling" in some works

Quantum Annealing<sup>22</sup> is a heuristic algorithm that operates within the principles of Adiabatic Quantum Computing<sup>23,24</sup>, particularly for solving optimization problems. In this regime, a given optimization task is encoded into a physical system described by a problem Hamiltonian  $H_P$ , so that the system's lowest energy state (ground state) corresponds to the solution of the original problem. Initially, the system is prepared in the ground state of another related physical system, described by the initial Hamiltonian  $H_0$ . Then, the system is slowly evolved into the target system  $H_P$  by tuning the parameters of the instantaneous Hamiltonian to turn  $H_0$  into  $H_P$  in a long enough time  $T$ . According to the adiabatic theorem<sup>25</sup>, if certain conditions hold, the system should remain in the ground state during the evolution and thus reach the ground state of  $H_P$  at the end, yielding a solution to the original problem. Mathematically, the evolution of the system is described by the following time-dependent Hamiltonian:

$$H(t) = \left(1 - \frac{t}{T}\right) H_0 + \frac{t}{T} H_P. \quad (1)$$

The quantum annealers which are provided by D-Wave and are applied in our research implement a problem Hamiltonian whose energy is expressed using a 2-local Ising model<sup>26</sup>:

$$H_P = \sum_{\langle i, i' \rangle \in E} J'_{i, i'} \sigma_i^z \sigma_{i'}^z + \sum_i h'_i \sigma_i^z, \quad (2)$$

where  $\sigma^z$  is a Pauli-Z operator acting on the  $i$ -th qubit, and  $J'_{i, i'}$  and  $h'_i$  are real values corresponding to pairwise couplings and the external magnetic field, respectively, and  $E$  is the graph of the processor topology. The initial Hamiltonian  $H_0$  is chosen to consist of a transverse magnetic field,  $H_0 = h_0 \sum_i \sigma_i^x$  where  $\sigma_i^x$  is the Pauli-X operator acting on the  $i$ -th qubit.

Finally, the results of quantum annealing are supposed to minimize the classical Ising problem in Eq. (3)

$$\min_{(s_1, \dots, s_n) \in \{-1, 1\}^N} \sum_{\langle i, i' \rangle \in E} s_i J'_{i, i'} s_{i'} + \sum_{i \in V} s_i h'_i \quad (3)$$

where  $s_i$  are spin variables  $s_i \in \{-1, 1\}$ ,  $J'_{i, i'}$  are couplings between spins, and  $h'_i$  are local fields. Such a problem can also be easily encoded in Quadratic Unconstrained Binary Optimization (QUBO) problem, namely:

$$\min_{(x_1, \dots, x_n) \in \{0, 1\}^N} \sum_{\langle i, i' \rangle \in E} x_i J_{i, i'} x_{i'} + \sum_{i \in V} x_i h_i \quad (4)$$

where  $x_i \in \{0, 1\}$  are binary variables, and  $s_i = 2x_i - 1$ .

In practice, many optimization problems, including our scheduling case, can be modelled as an integer linear program (ILP). The integer variables can be encoded into suitable binaries in various ways<sup>27,28</sup>. The constraints of the integer programs are taken into account with penalties<sup>29</sup>. The right choice of penalties, a nontrivial problem<sup>30–33</sup> itself. Although the size of the current quantum annealer is limited in terms of the number of qubits (in our case, approximately 5600 qubits and 40 thousands couplings between them organized into the Pegasus topology of QPU<sup>34</sup>), larger optimization problems, that do not fit quantum devices, can be solved via hybrid quantum-classical approach. D-Wave offers two hybrid classical-quantum solvers as a part of its service: BQM and CQM<sup>10,35</sup>.

The BQM solver inputs QUBO problems and solves them with a portfolio of classical heuristics. In the course of the process, certain subproblems are sent to the quantum processor. In the case of the CQM solver, the input is a constrained quadratic program, which can be an ILP. Its transformation to QUBO is performed within the solver. The handling of constraints with penalties is also done by the solver internally.

These solvers are proprietary and closed source; their details are hidden from the users. Nevertheless their operation can be understood according to D-Wave's white paper<sup>10</sup>. In particular, the data flow is described as follows. The solver reads the input problem. Then, it invokes a portfolio of heuristic solvers that run in parallel using classical CPUs and GPUs in a cloud computing environment. These heuristics contain a Quantum Module (QM), which can send queries to QPU. The quantum results help classical heuristic search to improve the quality of a current pool of solutions. After post-processing (removing duplicates, etc.), the results are forwarded to the user.

The hybrid solvers open the possibility of easily dealing with bigger-scale problems. For instance, CQM has recently been applied to the practical rescheduling problems in heterogeneous urban railway networks<sup>36</sup>.

### 3 AGV scheduling

The concept of industry 4.0<sup>13</sup> implies that AGV scheduling must be tied to the particular factory specifics. To tie our research directly to current business needs, we address a problem that arises in a production environment, i.e. the practice of an actual

operating factory. (Its identity and further details are confidential.) We model this particular environment, its configuration, and requirements, addressing the particular needs of the given factory. In this factory, there is a well-defined space where AGVs can maneuver. They are restricted to moving on dedicated "roads" (uni- or bidirectional) to reach ports, loading places, charging stations, etc. Here, the AGVs are controlled by a central system where their scheduling occurs.

Concerning a factory environment with limited space, an important issue with AGVs is the possibility of deadlocks, where several AGVs come to such a point that none of them can move forward because each of them is blocked by the others.<sup>17</sup> mentions various deadlock resolution methods:

1. Balancing the system workload, i.e. using workload-related dispatching rule<sup>37</sup>,
2. Controlling the traffic at intersections by semaphores<sup>38</sup>,
3. Introducing static or dynamic zones that a limited number of AGVs can occupy for a dynamic-zone strategy for vehicle-collision<sup>39</sup> prevention.

These deadlock resolution strategies can mostly be encoded as constraints to the ILP. We have opted for the last approach, i.e. dynamic zones. It is worth remembering that deadlock resolution in limited space is challenging and difficult, even with limited problem size (regarding the number of AGVs).

Our problem can also be understood in the standard metaphor of scheduling theory<sup>40</sup>: zones are *machines*, and AGVs are *jobs*. Each AGV has to visit a set of infrastructure elements in a given sequence: each job has to be processed by a set of machines in a prescribed order: this is a job-shop *Job Shop (Jm)* environment. Generalizations allowing for having multiple AGVs in a zone would result in a *Flexible Job Shop (FJc)* environment; this we will not consider here. We treat parts of the infrastructure that lie between zones (i.e. where conflicts are not expected) as buffers. The requirement of a minimal *headways* between AGVs leaving and entering zones and deadlock constraints on bidirectional "roads" (also termed as *lanes*) imply *blocking* constraints (*block*). The prescription of the initial availability of AGVs implies *release date* ( $r_j$ ) constraints. The minimal passing times of AGVs through particular resources are limited: *minimal processing times* ( $p_{jm}$ ) appear. In addition, *due dates* ( $d_j$ ) are also prescribed: the AGVs' tasks have to be completed in a given time. Finally, *permutation* (*prmu*) constraints arise, as AGVs cannot overtake on lanes between zones. Recirculation (*rcrc*), if a given AGV can visit the same zone multiple times during the trip, could also be considered but will not be addressed here as it does not occur in the particular factory we model.

The objective is to ensure that the AGVs finish their travels as soon as possible, considering certain priorities. Hence, the objective is the *travel completion time*, the weighted sum of completion times of each AGV. We shall refer to this as completion time in what follows. With the standard notation of scheduling theory, our problem falls in the class  $(J_m | r_j, p_{jm}, d_j, block, prmu | \sum_j w_j C_j)$ .

The objective is the weighted sum of completion times<sup>17</sup>. The weights reflect the priorities of AGVs. We assume that AGVs' tasks and paths (represented by the colour lines in Fig. 1) are pre-defined as input for our problem. Each time these inputs are changed, a new optimization problem is created and recomputed. Such changes in the input can be caused e.g. by disturbances in the AGV traffic.

Fig. 1 displays an example of the considered topologies. This setup closely resembles the situation in the considered real-life factory (it is distorted to maintain confidentiality). AGVs paths (color lines) are as follows:

- bidirectional lanes (e.g. between  $s_5$  and  $s_6$  in Fig. 1),
- uni-directional lanes,
- zones<sup>39</sup> the locations where conflicts are possible according to the given (predefined) paths, i.e. where AGVs paths split, join, or where uni-directional lanes start or end.

To avoid collisions, we assume that only one AGV can occupy each zone at a given time (This limitation can be lifted in a more elaborate model by increasing the allowed number of AGVs within the zone and introducing some local traffic conditions<sup>38</sup>.)

### 3.1 AGV scheduling: algorithm

The practical AGVs scheduling will be performed via the following algorithm triggered at each change of input parameters.

#### Fixed inputs

1.  $J$  - set of AGVs;
2.  $w_j$  - priority weights (as the part of *total weighted completion time* objective);

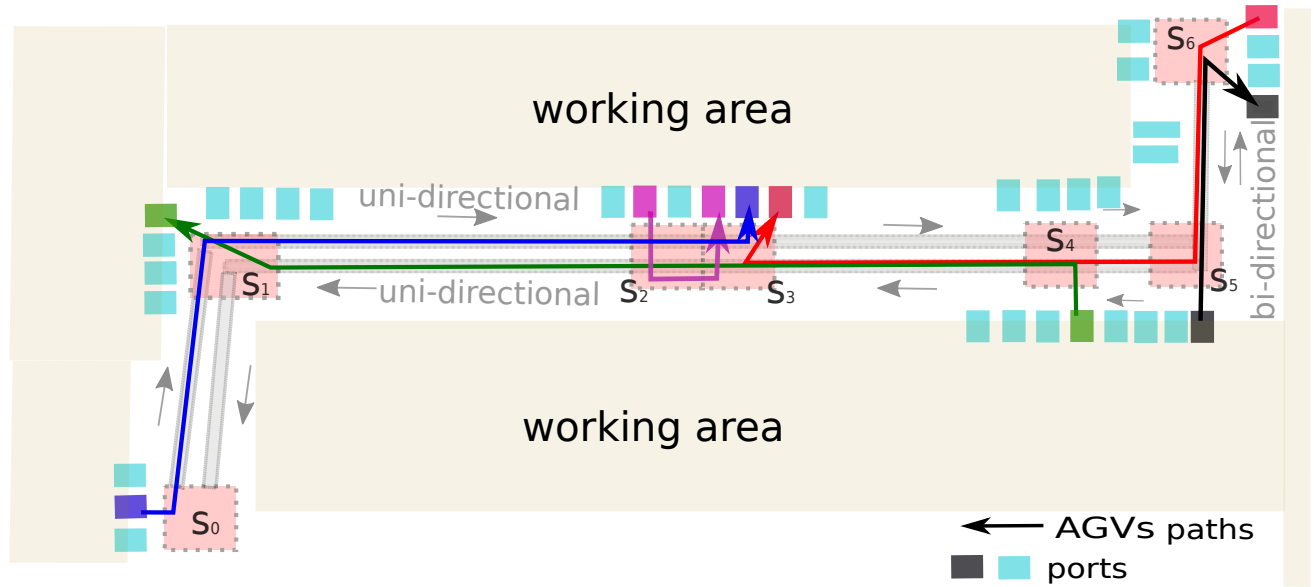


**Figure 1.** Example of the AGV scheduling problem given pre-defined AGVs paths as colour lines. First, AGVs are routed to travel between ports, what is the input to our algorithm. The goal of the algorithm is to timetable AGVs to avoid collisions at zones. In our case zones  $s_0, \dots, s_6$  are allegorically assigned spatial areas where AGVs paths intercept start or active ports are located. AGVs paths in terms of zones are **AGV**  $s_0, s_1, s_2, s_3$ , **AGV**  $s_4, s_3, s_2, s_1$ , **AGV**  $s_6, s_5, s_4, s_3$  **AGV**  $s_5, s_6$  and **AGV**  $s_2, s_3$

3.  $d_{\max}$  - the parameter determining the time window, *due time*, +can be computed from this parameter;
4. topology of the network as in Fig. 1, containing:
  - uni-directional double lanes,
  - bidirectional single lanes (imposing *blocking* constraints);
5. minimal headways between two subsequent AGVs, this is a parameter of *blocking* constraints.

#### Variable inputs

1. starting points of AGVs in time and space,
2. AGVs destinations and paths (from this, the sequence of machines will be determined);
3. nominal speeds of AGVs, *processing time* constraints can be formulated based on these parameters.

#### Processing

1. from paths of AGVs create zones where conflicts are possible; see Fig. 1,
2. define AGVs paths by the sequence of zones e.g.  $S_j = \{s_{j,1}, s_{j,2} \dots s_{j,\text{end}-1}, s_{j,\text{end}}\}$ , e.g. see caption of Fig. 1;
3. given initial conditions, compute the lowest possible entering and leaving times of each AGV at the zones, assuming there are no collisions between the given AGV and all other AGVs;
4. encode the problem into ILP: entering and leaving times of AGVs at the zones are integer decision variables, and there are binary order variables determining which AGV leaves a zone first. (A relaxation of the integer constraint on time variables yields a mixed integer program that is also meaningful but not considered here, as quantum devices support integers. In addition, our computational experience shows that the relaxation of the integer constraints on time variables and using a MILP solver does not significantly improve computational time when using CPLEX; the real difficulty is encoded in the order variables.) Lower limits of these variables are determined in point 3 while upper limits are determined by lower limits and model parameter  $d_{\max}$ , encode constraints and objective;
5. solve the problem using a chosen solver (classical, quantum, hybrid, etc.).

## Output

1. conflict-free timetable of AGVs encoded as entering and leaving times of AGVs at zones, or correspondingly the order of AGVs therein.

Steps 1 - 3 in **processing** are pre-processing steps. The higher computational effort is required in step 5, which deals with optimization. Hence, the analysis of the computation process (both quantum and classical) will refer to step 5 of the algorithm. Importantly, the optimization results (values of order variables uniquely defining the order of AGVs at each zone while the traffic beyond zones is conflict-free) can be directly fed into the application programming interface (API) of the operation control software system of the factory we have modeled.

### 3.2 AGV scheduling: ILP model

Here, we provide the details of the model in step 4 of the algorithm, given that step 5 will be handled in Section 4.

**Decision variables** include the integer times when AGVs are entering and leaving zones are denoted by  $t_{in/out}(j, s)$ . As floating point numbers cannot be treated easily, we use integer time variables  $t_{in/out}(j, s) \in \mathbb{N}$ . The time window constraints<sup>17</sup>, implies that each of these variables fit into the time window of length  $d_{max}$ , namely:

$$v_{in/out}(j, s) \leq t_{in/out}(j, s) \leq v_{in/out}(j, s) + d_{max}. \quad (5)$$

where  $v_{in/out}(j, s)$  are lower limits computed by assuming the nominal speed of  $j$ 'th AGV and assuming no conflicts (collisions) with other AGVs, according to<sup>40</sup>. The  $d_{max}$  parameter imposes *due time* constraints, while lower limits are tied to *release date* constraints. Let  $|S|$  be the number of zones in a particular optimization problem, and  $|J|$  the number of AGVs therein.

To determine the order of AGVs at zones, we introduce binary order variables.

- For zone  $s$  passed by AGVs  $j$  and  $j'$  we have:

$$y_{in/out}(j, j', s) \in \{0, 1\} \quad (6)$$

which is equal to 1 iff  $j$  enters / leaves zone  $s$  before  $j'$ , as the order of AGVs cannot be changed at the zone by assumption; obviously:

$$y_{in/out}(j, j', s) = 1 - y_{in/out}(j', j, s). \quad (7)$$

- For a bidirectional lane (joining zones  $s$  and  $s'$ ) used by AGV  $j$  heading in one direction and AGV  $j'$  heading in the opposite direction, we assign the following order variable:

$$z(j, j', s, s') \in \{0, 1\}, \quad (8)$$

which is equal to 1 iff  $j$  enters such lane (bounded by zone  $s$  and  $s'$ ) before  $j'$ , and zero otherwise, hence,

$$z(j, j', s, s') = 1 - z(j', j, s, s'). \quad (9)$$

As for the number of variables observe that if an AGV passes a zone, there are two  $t$  variables (c.f. Eq. (5)); for the AGV entering and leaving the zone. As not all AGVs pass through all zones, we have

$$\#t \leq 2|J||S|. \quad (10)$$

Concerning order variables, for each pair of AGVs passing a zone there is a pair of these ( $y_{in}$  and  $y_{out}$ ). However, the order of AGVs cannot change in a zone (this will be enforced by constraints in Eq. (22)), a single order variable per zone and AGVs' pair suffices; there are  $|J|(|J| - 1)/2$  such pairs. Further, if hypothetically the whole topology consisted of bidirectional lanes, we had  $\#z = \#y$ . In a more general layout, inequality  $\#z \leq \#y$  holds. Hence,

$$\#y \leq \frac{|J|(|J| - 1)|S|}{2}, \quad \#z \leq \frac{|J|(|J| - 1)|S|}{2}, \quad \text{and} \quad \#y + \#z + \#t \ll |J|(|J| - 1)|S| + 2|J||S|. \quad (11)$$

For topologies with most uni-directional lanes (as in our example in Section 3.1), we have  $\#z \ll \#y$ , which leads to the following approximation:

$$\#y + \#z + \#t \ll \frac{|J|(|J| - 1)|S|}{2} + 2|J||S|. \quad (12)$$



**Objective** is defined as the weighted sum of completion times<sup>17</sup>, namely:

$$f = \sum_{j \in J} w_j \frac{t_{\text{out}}(j, s_{j,\text{end}})}{d_{\text{max}}}. \quad (13)$$

Here  $s_{j,\text{end}}$  is the last zone of the path of  $j$  AGV, and  $w_j$  is the weight tied to the priority of such AGV. (We assume that the AGV's path is conflict-free after leaving the last zone.) This can be referred to as the *total completion time* objective.

**Constraints.** The *minimal passing time* constraint (mpt) of AGVs between subsequent zones can be computed from the problem topology and AGVs speeds. For any pair of subsequent zones  $(s, s')$  on the route of AGV  $j$  we require:

$$t_{\text{in}}(j, s') \geq t_{\text{out}}(j, s) + \tau^{\text{pass}}(j, s, s'), \quad (14)$$

see Fig. 2 (upper panel). In our model, zones are considered as bottleneck areas. Hence, we allow waiting of AGVs in the buffer before the zone entrance, yielding  $\geq$  sign in Eq. (14).

The *minimal headway* constraint (mh) is the model input that determines minimal time spacing between two subsequent AGVs. In detail, consider two AGVs  $j, j'$  heading in the same direction. Let  $s^*, s, s'$  be the sequence of subsequent zones they both pass. Then:

$$t_{\text{out}}(j', s) + M \cdot y_{\text{out}}(j', j, s) \geq t_{\text{out}}(j, s) + \tau^{\text{headway}}(j, j', s, s'), \quad (15)$$

see Fig. 2 (lower panel), and analogously

$$t_{\text{in}}(j', s) + M \cdot y_{\text{in}}(j', j, s) \geq t_{\text{in}}(j, s) + \tau^{\text{headway}}(j, j', s^*, s). \quad (16)$$

Here  $M$  is a large enough number for inequality to always hold for  $y(j', j, s) = 1$  (we used so called “big M encoding”). If  $s$  does not have a successor in the sequence, we do not consider Eq. (15). Analogously, if  $s$  does not have the predecessor, we do not consider Eq. (16).

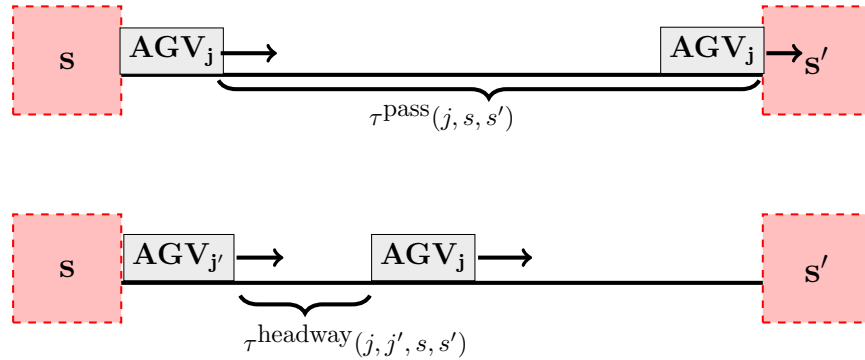


**Figure 2.** Illustration of *minimal passing time* (upper panel) and *headway* (lower panel) Eq. (14)

The *deadlock* on bidirectional lane constraint (d) is defined as follows. Let the pair  $(s, s')$  be two zones connected by the single bidirectional lane and  $j$  and  $j'$  be two AGVs first going  $s \rightarrow s'$  and the second  $s \leftarrow s'$ . Then:

$$t_{\text{out}}(j', s') + M \cdot z(j', j, s', s) \geq t_{\text{in}}(j, s') \quad (17)$$

and

$$z(j, j', s, s') = y_{\text{in}}(j, j', s) = y_{\text{in}}(j, j', s') \quad (18)$$

Equation (18) yields that the order of AGVs heading in opposite directions cannot change between zones  $s, s'$  (including zones itself), as they cannot meet at the bidirectional lane, which would lead to the deadlock.

In the *zone constraint* (zc), we assume that the zone can be occupied only by one AGV at a time. This is to avoid collisions within the zone. Hence, AGV  $j'$  can enter the zone after  $j$  leaves it (provided  $j$  is first on the zone, i.e.  $y_{\text{in}}(j', j, s) = 0$ ):

$$t_{\text{in}}(j', s) + M \cdot y_{\text{in}}(j', j, s) \geq t_{\text{out}}(j, s) \quad (19)$$

Then we also have to include minimal passing time over the zone  $\tau^{\text{zone}}$

$$t_{\text{out}}(j, s) \geq t_{\text{in}}(j, s) + \tau^{\text{zone}}(j, s). \quad (20)$$

In the scheduling theory language: the assumption that the zone can be occupied by one AGV only defines the *job shop* machine environment, and the prescription of the passing time over zones imposes *processing time* constraints.

As AGVs are, in general, moving with similar speed, we assume that they cannot overtake both on lanes and zones. This *no overtake* (no) constraint requires the order of such AGVs to be maintained. (This is the *permutation constraint*.) In detail, let  $j$  and  $j'$  be a pair of AGVs heading in the same direction, passing the sequence of zones:  $s_1, s_2, \dots, s_k$ . Then:

$$y(j, j', s_{1\text{out}}) = y(j, j', s_{2\text{out}}) = \dots = y(j, j', s_{k\text{out}}) \quad (21)$$

(Note that if the route of two AGVs splits and joins later, the condition in Eq. (21) has to be modified).

As mentioned before, we also assume that AGVs cannot overtake within a zone:

$$y_{\text{in}}(j, j', s) = y_{\text{out}}(j, j', s). \quad (22)$$

Let us now estimate the number of constraints. The *minimal passing time* (mpt) constraint, there is a single inequality as in Eq. (14) for each AGV and each zone passed by this AGV. Then, taking the upper limit of each AGV passing each zone, we have

$$\#_{\text{mpt}} \leq |J||S|. \quad (23)$$

The *minimal headway* (mh) constraints are required for each pair of AGVs following each other at each zone. There are roughly  $|J|^2/2$  such pairs. To obtain an upper limit we consider all AGVs passing all zones. Then, for each AGV in the pair and each zone, we have one constraint from Eq. (15) and one from Eq. (16);

$$\#_{\text{mh}} \leq 2 \frac{|J|^2}{2} |S| = |J|^2 |S|. \quad (24)$$

Analogously, we would expect from Eq. (17) the same limit for the number of *deadlock* (d) constraints;

$$\#_{\text{mh}} + \#_{\text{d}} \leq 2|J|^2 |S|. \quad (25)$$

To approximate the number of *zone constraints* (zc), the upper limit is obtained again with the hypothetical assumption that all AGVs pass all zones. Then for each zone and each AGV we have  $|J| - 1$  inequalities from Eq. (19) and one inequality from Eq. (20), yielding

$$\#_{\text{zc}} \leq |J|^2 |S|. \quad (26)$$

Hence, the number of *minimal passing time* (mpt) constraints (see Eq. (23)) is linear in  $|J|$ , while the number of all other constraints (zc, mh, d) is quadratic in  $|J|$ . Then, for a large enough  $|J|$ , we can assume:

$$m = \#_{\text{mpt}} + \#_{\text{zc}} + \#_{\text{mh}} + \#_{\text{d}} \approx \#_{\text{zc}} + \#_{\text{mh}} + \#_{\text{d}} \leq 3|J|^2 |S|, \quad (27)$$

Finally, the number of **no overtake** (no) constraints in Eq. (21)

$$\#_{\text{no}} \leq \frac{|J|^2 |S|}{2} \quad (28)$$

is also expected to be linear in  $|S|$  and quadratic in  $|J|$ .

Altogether the problem size (in terms of the number of constraints and binary variables) scales linearly in the number of zones  $|S|$  and quadratically in the number of AGVs  $|J|$ . The quadratic scaling can cause difficulties when applying the ILP model to a large number of AGVs. As such, this AGV problem seems to be a good use-case for the quantum approach described at the beginning of this section.



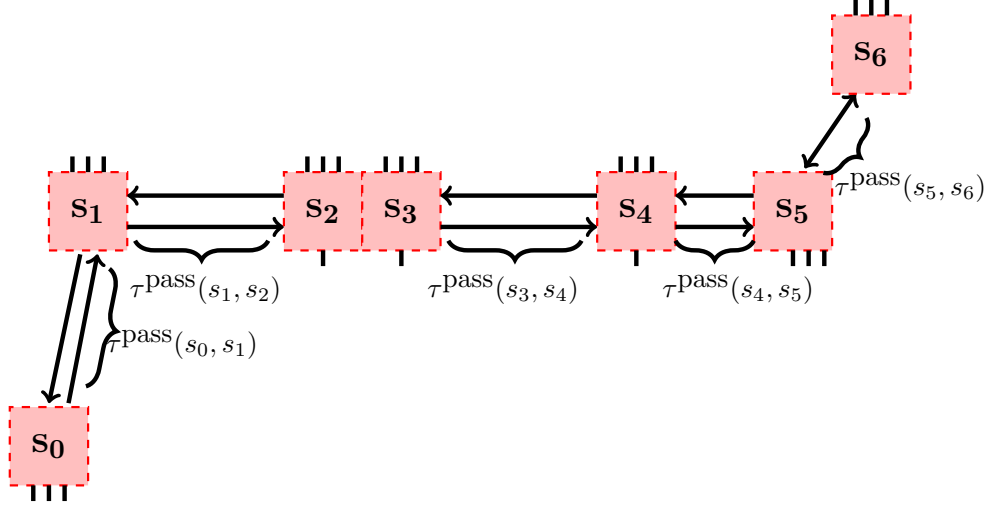


**Figure 3.** Example network with 7 zones derived from Fig. 1

$ J  /  S  / d_{\max}$	actual ILP			upper limit		
	n.o. vars int / bin	n.o. equalities	n.o. inequalities	n.o. vars Eq. (12)	equalities Eq. (28)	inequalities Eq. (27)
2 / 4 / 10	16 12/4	4	16	20	16	32
4 / 4 / 10	36 20/16	10	34	56	62	124
6 / 7 / 40	78 38/40	32	80	189	252	504
7 / 7 / 40	118 48/70	55	127	245	343	686
12 / 7 / 40	596 102/494	429	766	630	1008	2016
15 / 7 / 40	696 118/576	495	883	945	1575	3150

**Table 1.** Sizes of ILPs of the analyzed AGV problems. The notion of upper limits is described in Section 3.2. We have approximately 2 constraints per variable (equality and inequality), what makes the the problem sparse in comparison with railway counter example in<sup>36</sup>.

## 4 Computational results and discussion

For numerical calculations we used examples of problems similar to those presented in Fig. 1, but with different numbers of AGVs and zones. This is a typical setting in an industrial system, as various AGVs are in traffic at various times, and collision zones form dynamically. As a typical example of the particular parameter setting with 7 zones see Fig. 3. The actual values of parameters can be read from the topology, AGVs' speeds, and zone locations. The example with 7 zones and 7 AGVs will be discussed in more detail in Appendix B.

From an optimization point of view, one of our goals is to examine the scaling of the problems' computational time and number of variables and constraints with the size of the problem in terms of  $|J|$  and  $|S|$  (namely the number of AGVs and zones). We start with 2 AGVs and 4 zones and end with 15 AGVs and 7 zones. The sizes of the instances we have solved are tabulated in Tab. 1. Referring to somehow analogous problem in railways in<sup>36</sup> with 3 to 5,5 constraints per variable the AGV problem is much more sparse (approximately 2 constraints per variable). Such less dense problem is more probable to be better handled on the quantum device, where the embedding on the device with limited degree connectivity is performed.

All classical (that is not quantum) calculations were performed on the consumer-grade computer described in Tab. 2, and quantum calculations were performed on DWave's Advantage\_systems6.2 quantum annealer, whose physical properties are described in<sup>34</sup>. In short, the quantum device has over 5600 qubits and 40 thousand couplings between them, organized into the Pegasus topology of QPU. Concerning pure quantum computing, we were able to fit to real quantum device only first two smallest problems, from Table. 1. The larger of 36 ILP variables and 44 ILP constrains (equalities and inequalities) was converted into 268 qubits Ising problem with 2644 (quadratic) couplings between. However, even for these two small problems we did not achieve the feasible solution. From this, we can conclude that quantum annealers are too small and too prone to

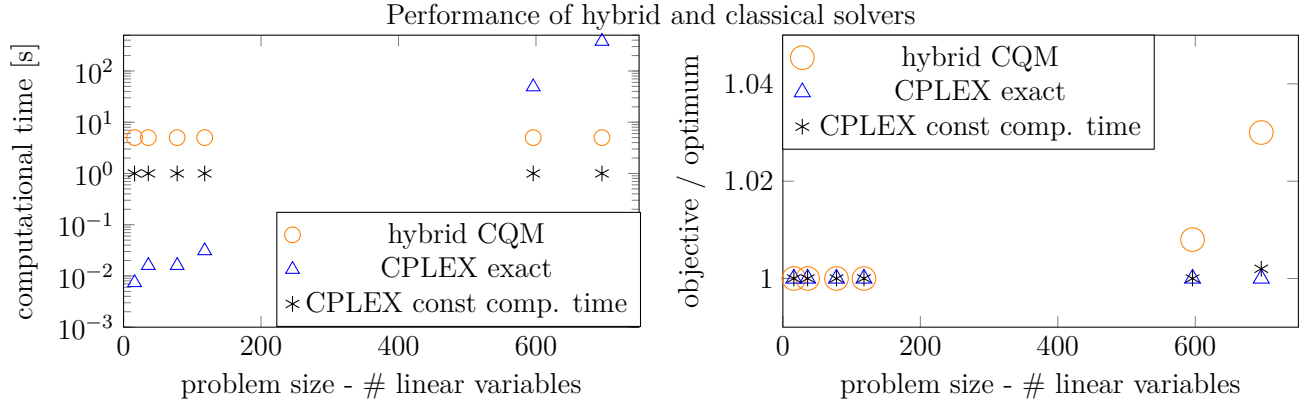


**Figure 4.** Comparison of performance of Classical CPLEX exact and approximate (achieved by setting constant computational time) with hybrid quantum-classical solver, CQM in particular. All presented solutions were feasible. As concerning BQM feasible solutions were found only for small instances.

OS	Windows 10 Pro N
Type	64 bits
CPU	11th Gen Intel(R) Core(TM) i5-11600K @ 3.90GHz
RAM	32 GB
GPU	Intel(R) UHD Graphics 750

**Table 2.** Technical specifications of the classical computer used for computations.

errors, and hence for more accurate solutions of larger problem we opt for hybrid quantum - classical solvers.

Our first approach was to use the BQM solver. In order to do so, the ILP has to be converted to QUBO. Appendix A describes the details of this transcription. The constraints were taken into account with penalties using ad-hoc penalty coefficients. We have found that except for the smallest problems, the BQM solver does not return high-quality solutions (see Fig. 6, right panel). Notably, the solutions were not feasible: a more advanced and systematic determination should replace our ad-hoc choice of the penalty coefficients. As this issue is handled in the CQM solver, we switched to that one. Indeed, the CQM hybrid solver, which is convenient also because it accepts ILPs directly, has always provided some feasible solutions in our problems.

We have therefore made a comparison of 3 approaches: the exact CPLEX ILP solver which always solves the problem to optimality, an approximate CPLEX solution, achieved by setting constant computational time for CPLEX solver, and the CQM hybrid solver as an approximate heuristic. Our comparison is summarized in Fig. 4. In terms of computational time, CQM has outperformed the classical exact CPLEX solver for large problems (596 and 696 linear variables). It has to be noted

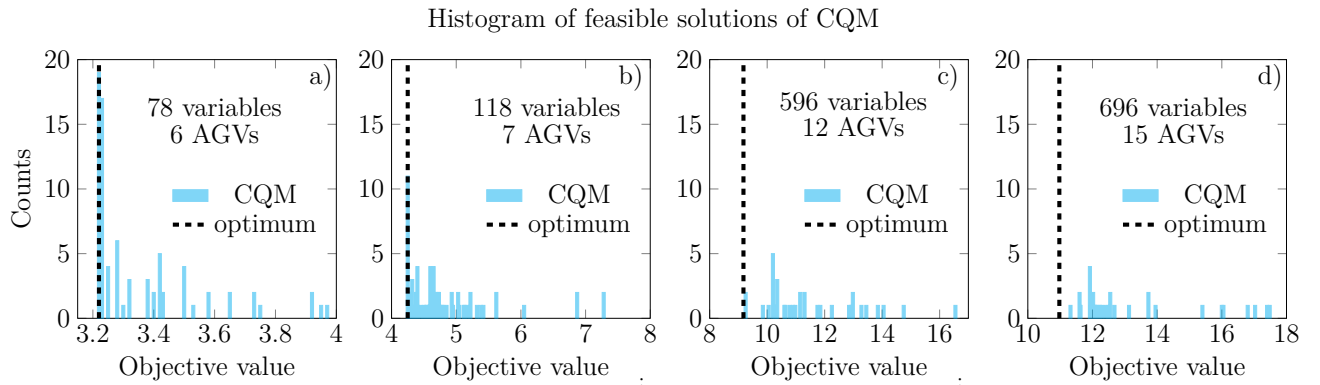


**Figure 5.** Histograms of objectives of feasible CQM solutions for various problem sizes: 6 AGVs a), 7 AGVs b), 12 AGVs c), 15 AGVs d). For each run approx hundred of samples were returned. Histogram spreads are measured by standard deviation (std): 6 AGVs std = 0.19, 7 AGVs std = 0.68, 12 AGVs std = 1.66, 15 AGVs std = 2.08.

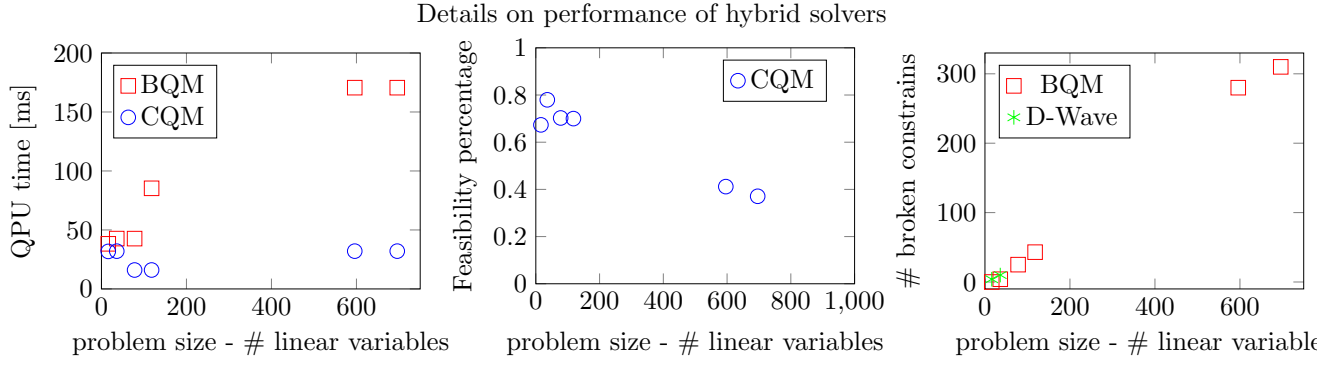


**Figure 6.** Details of hybrid solvers. The QPU time is in the left panel, and the number of broken constraints of the solution is in the right panel. Observe that the output of the CQM solver was satisfactory, which was not the case in the BQM solver, especially for large problems.

that in each of the CQM computations, a nonzero QPU time was reported (see Fig. 6, left panel), indicating that the QPU was active during the calculation. The largest problem was of 15 AGVs and 7 zones, which is the sound size concerning the real live factory environment. As for the quality of the solutions, slightly higher objective value than the exact solution. This overview shows that the CPLEX approximate solver, performing all computations in 1 second, is fast enough for almost online scheduling and dynamics response of our algorithm. Hence, such results would be admissible for practical application in real-life factories. In the future, when better quantum annealers will be available, they may become more efficient than classical heuristics. Concerning railway counterpart problem in <sup>36</sup> and analogous real live problems of 817 variables and over 3000 constraints the performance of the CQM solver therein could compete only with exact CPLEX in terms of computational time but at larger cost of the solution quality than in the AGV case.

As the CQM solver returns multiple feasible solutions at a time, in Fig. 5 we present the histograms of these, for problems of various sizes. Observe that for small problems, the results concentrate around the optimum, while for large problems, the histogram spreads towards higher-than-optimum objective values. It is important to note that even for large problems there are multiple feasible and potentially valuable solutions obtained. The results with the CQM solver are competitive and illustrate an efficient application of hybrid algorithms. The details of a particular case and its solutions, including a detailed comparison of classical and different quantum solutions are presented in Appendix B.

For the largest problem of 15 AGVs and 7 zones (696 linear variables), the problem is still tractable using classical heuristics. As we expect the size of the problem to scale quadratically with the number of AGVs, other heuristics may be required to handle larger problems in expanding industrial environments; a hybrid quantum-classical approach may be one of these. This however would also require the improvement of the hybrid solvers as the feasibility percentage of CQM decreases with the problem size, as it can be observed in Fig. 6, middle panel. If the linear scaling between feasibility percentage and the number of linear variables holds, the biggest problems that can be solvable using the current CQM can have approximately up to 1000 variables.

## 5 Conclusions

In this research, we have demonstrated the utility of a hybrid quantum-classical approach for a close-to-real-life AGVs scheduling problem that can be implemented in a real factory environment. We have not yet demonstrated *quantum advantage*, but the results of one of the hybrid quantum-classical approaches are close to those of CPLEX, which is widely recognized as the benchmark classical solver. As such hybrid approaches are expected to improve in the near future, we may be on the edge of *quantum advantage*. While larger problems of hundreds of AGVs that are expected to arise from the developments of the concept of industry 4.0 (yielding several thousands of variables in our model) may remain out of the range of classical algorithms, future hybrid quantum-classical algorithms can be expected to have the potential to cope with them.

The CQM solver even for large problems provides the spectrum of distinguishable solutions, that can be the input to multi cases DSS system or sophisticated stochastic scheduling approach. Besides, CPLEX (with limited time) is faster and closer to optimality it provides only one solution. The experience with BQM underlines the importance of systematic penalty determination<sup>33,32</sup>.

## Data availability

The code and the data used for generating the numerical results can be found in [https://github.com/iitis/AGV\\_quantum](https://github.com/iitis/AGV_quantum)

## Acknowledgements

The research was supported by the Foundation for Polish Science (FNP) under grant number TEAM NET POIR.04.04.00-00-17C1/18-00 (BG, ZP, ŁP); National Science Centre, Poland under grant number 2022/47/B/ST6/02380 (KD), and under grant number 2020/38/E/ST3/00269 (TŚ), and by the Ministry of Culture and Innovation and the National Research, Development and Innovation Office within the Quantum Information National Laboratory of Hungary (Grant No. 2022-2.1.1-NL-2022-00004) (MK). S.D. acknowledges support from the John Templeton Foundation under Grant No. 62422. For the purpose of Open Access, the authors have applied a CC-BY public copyright license to any Author Accepted Manuscript (AAM) version arising from this submission.

## Author contributions statement

Z.P., B.G., S.D., K.D. - conceptualization, K.D., T.Ś. - preparing experiments, T.Ś. - running experiments, K.D., Z.P., Ł.P., M.K., B.G., S.D. - data analysis, K.D., M.K., T.Ś. - manuscript writing, Z.P., Ł.P., B.G., S.D. - manuscript supervision. All authors reviewed the manuscript.

## References

1. Shor, P. W. Algorithms for quantum computation: discrete logarithms and factoring. In *Proceedings 35th annual symposium on foundations of computer science*, 124–134, DOI: <https://doi.org/10.1109/SFCS.1994.365700> (IEEE, 1994).
2. Preskill, J. Quantum computing and the entanglement frontier. *arXiv preprint arXiv:1203.5813* (2012). <https://arxiv.org/abs/1203.5813>.
3. Preskill, J. Quantum computing in the NISQ era and beyond. *Quantum* **2**, 79, DOI: <https://doi.org/10.22331/q-2018-08-06-79> (2018).
4. Brooks, M. Beyond quantum supremacy: the hunt for useful quantum computers. *Nature* **574**, 19–21, DOI: <https://doi.org/10.1038/d41586-019-02936-3> (2019).
5. Arute, F. *et al.* Quantum supremacy using a programmable superconducting processor. *Nature* **574**, 505–510, DOI: <https://doi.org/10.1038/s41586-019-1666-5> (2019).
6. Domino, K. *et al.* Quantum annealing in the NISQ era: railway conflict management. *Entropy* **25**, 191, DOI: <https://doi.org/10.3390/e25020191> (2023).
7. Vikstål, P. *et al.* Applying the Quantum Approximate Optimization Algorithm to the Tail-Assignment Problem. *Phys. Rev. Appl.* **14**, 034009, DOI: <https://doi.org/10.1103/PhysRevApplied.14.034009> (2020).
8. Geitz, M., Grozea, C., Steigerwald, W., Stöhr, R. & Wolf, A. Solving the Extended Job Shop Scheduling Problem with AGVs—Classical and Quantum Approaches. In *International Conference on Integration of Constraint Programming, Artificial Intelligence, and Operations Research*, 120–137, DOI: <https://doi.org/10.1007/978-3-030-19212-9> (Springer, 2022).
9. Katzgraber, H. Searching for applications of quantum computing in industry. *Bull. Am. Phys. Soc.* (2024). <https://meetings.aps.org/Meeting/MAR24/Session/Y49.1>.
10. D-Wave Systems Inc. Hybrid Solver for Quadratic Optimization [WhitePaper] (2022). <https://www.dwavesys.com/media/soxph512/hybrid-solvers-for-quadratic-optimization.pdf>, visited 2023.08.31.
11. Rossit, D. A., Tohmé, F. & Frutos, M. Industry 4.0: smart scheduling. *Int. J. Prod. Res.* **57**, 3802–3813, DOI: <https://doi.org/10.1080/00207543.2018.1504248> (2019).
12. Stock, T. & Seliger, G. Opportunities of sustainable manufacturing in industry 4.0. *procedia CIRP* **40**, 536–541, DOI: <https://doi.org/10.1016/j.procir.2016.01.129> (2016).
13. Luo, Y., Duan, Y., Li, W., Pace, P. & Fortino, G. A novel mobile and hierarchical data transmission architecture for smart factories. *IEEE Transactions on Ind. Informatics* **14**, 3534–3546, DOI: <https://doi.org/10.1109/TII.2018.2824324> (2018).
14. Zhong, M., Yang, Y., Dessouky, Y. & Postolache, O. Multi-AGV scheduling for conflict-free path planning in automated container terminals. *Comput. & Ind. Eng.* **142**, 106371, DOI: <https://doi.org/10.1016/j.cie.2020.106371> (2020).

15. Qiu, L., Hsu, W.-J., Huang, S.-Y. & Wang, H. Scheduling and routing algorithms for AGVs: a survey. *Int. J. Prod. Res.* **40**, 745–760, DOI: <https://doi.org/10.1080/00207540110091712> (2002).
16. Vivaldini, K. C., Rocha, L. F., Becker, M. & Moreira, A. P. Comprehensive review of the dispatching, scheduling and routing of AGVs. In *CONTROLO'2014—proceedings of the 11th Portuguese conference on automatic control*, 505–514 (Springer, 2015).
17. Le-Anh, T. *Intelligent control of vehicle-based internal transport systems*. 51 (Erasmus University Rotterdam, 2005). <http://hdl.handle.net/1765/6554>.
18. Sabuncuoglu, I. & Bayız, M. Analysis of reactive scheduling problems in a job shop environment. *European Journal of Operational Research* **126**, 567–586, DOI: [https://doi.org/10.1016/S0377-2217\(99\)00311-2](https://doi.org/10.1016/S0377-2217(99)00311-2) (2000).
19. Li, G., Li, X., Gao, L. & Zeng, B. Tasks assigning and sequencing of multiple AGVs based on an improved harmony search algorithm. *J. Ambient Intell. Humaniz. Comput.* **10**, 4533–4546, DOI: <https://doi.org/10.1007/s12652-018-1137-0> (2019).
20. Haba, R., Ohzeki, M. & Tanaka, K. Travel time optimization on multi-AGV routing by reverse annealing. *arXiv preprint arXiv:2204.11789* (2022). <https://arxiv.org/abs/2204.11789>.
21. Pirnay, N., Ulitzsch, V., Wilde, F., Eisert, J. & Seifert, J.-P. An in-principle super-polynomial quantum advantage for approximating combinatorial optimization problems via computational learning theory. *arXiv preprint arXiv:2212.08678* (2024). <https://arxiv.org/abs/2212.08678>.
22. Apolloni, B., Carvalho, C. & De Falco, D. Quantum stochastic optimization. *Stoch. Process. their Appl.* **33**, 233–244, DOI: [https://doi.org/10.1016/0304-4149\(89\)90040-9](https://doi.org/10.1016/0304-4149(89)90040-9) (1989).
23. Kadowaki, T. & Nishimori, H. Quantum annealing in the transverse Ising model. *Phys. Rev. E* **58**, 5355, DOI: <https://doi.org/10.1103/PhysRevE.58.5355> (1998).
24. Farhi, E., Goldstone, J., Gutmann, S. & Sipser, M. Quantum Computation by Adiabatic Evolution. *arXiv preprint quant-ph/0001106* (2000). <https://arxiv.org/abs/quant-ph/0001106>.
25. Tanaka, S., Tamura, R. & Chakrabarti, B. K. *Quantum spin glasses, annealing and computation* (Cambridge University Press, 2017).
26. Lucas, A. Ising formulations of many NP problems. *Front. Phys.* **2**, 5, DOI: <https://doi.org/10.3389/fphy.2014.00005> (2014).
27. Karimi, S. & Ronagh, P. Practical integer-to-binary mapping for quantum annealers. *Quantum Inf. Process.* **18**, 1–24, DOI: <https://doi.org/10.1007/s11128-019-2213-x> (2019).
28. Tamura, K., Shirai, T., Katsura, H., Tanaka, S. & Togawa, N. Performance comparison of typical binary-integer encodings in an ising machine. *IEEE Access* **9**, 81032–81039 (2021).
29. Glover, F., Kochenberger, G., Hennig, R. & Du, Y. Quantum bridge analytics i: a tutorial on formulating and using qubo models. *Annals Oper. Res.* **314**, 141–183 (2022).
30. Karimi, S. & Ronagh, P. A subgradient approach for constrained binary optimization via quantum adiabatic evolution. *Quantum Inf Process.* **16**, DOI: <https://doi.org/10.1007/s11128-017-1639-2> (2017).
31. Gusmeroli, N. & Wiegele, A. EXPEDIS: An exact penalty method over discrete sets. *Discret. Optim.* **44**, 100622, DOI: <https://doi.org/10.1016/j.disopt.2021.100622> (2022).
32. Quintero Ospina, R. A., Zuluaga, L., Terlaky, T. & Vera, J. Polyhedral structure of penalty constants in quadratic unconstrained binary optimization and applications to quantum computing. In *APS March Meeting Abstracts*, vol. 2023, B70–007 (2023). <https://ui.adsabs.harvard.edu/abs/2023APS..MARB70007Q>.
33. García, M. D., Ayodele, M. & Moraglio, A. Exact and sequential penalty weights in quadratic unconstrained binary optimisation with a digital annealer. In *Proceedings of the Genetic and Evolutionary Computation Conference Companion*, 184–187, DOI: <https://doi.org/10.1145/3520304.3528925> (2022).
34. D-Wave Systems Inc. QPU-Specific Physical Properties: Advantage\_system6.2 (2023).
35. D-Wave Systems Inc. Hybrid Solver for Constrained Quadratic Model [WhitePaper] (2022). [https://www.dwavesys.com/media/rldh2ghw/14-1055a-a\\_hybrid\\_solver\\_for\\_constrained\\_quadratic\\_models.pdf](https://www.dwavesys.com/media/rldh2ghw/14-1055a-a_hybrid_solver_for_constrained_quadratic_models.pdf), visited 2023.08.31.
36. Koniorczyk, M., Krawiec, K., Botelho, L., Bešinović, N. & Domino, K. Solving rescheduling problems in heterogeneous urban railway networks using hybrid quantum-classical approach. *arXiv preprint arXiv:2309.06763* (2023). <https://arxiv.org/abs/2309.06763>.

37. Kim, C., Tanchoco, J. & Koo, P.-H. AGV dispatching based on workload balancing. *Int. J. Prod. Res.* **37**, 4053–4066, DOI: <https://doi.org/10.1080/002075499189925> (1999).
38. Evers, J. J. & Koppers, S. A. Automated guided vehicle traffic control at a container terminal. *Transp. Res. Part A: Policy Pract.* **30**, 21–34, DOI: [https://doi.org/10.1016/0965-8564\(95\)00011-9](https://doi.org/10.1016/0965-8564(95)00011-9) (1996).
39. Ho, Y.-C. A dynamic-zone strategy for vehicle-collision prevention and load balancing in an AGV system with a single-loop guide path. *Comput. industry* **42**, 159–176, DOI: [https://doi.org/10.1016/S0166-3615\(99\)00068-8](https://doi.org/10.1016/S0166-3615(99)00068-8) (2000).
40. Pinedo, M. L. *Scheduling*, vol. 29 (Springer, 2012). <https://doi.org/10.1007/978-1-4614-2361-4>.
41. Darlay, J., Brauner, N. & Moncel, J. Dense and sparse graph partition. *Discret. Appl. Math.* **160**, 2389–2396, DOI: <https://doi.org/10.1016/j.dam.2012.06.004> (2012).

## A QUBO model

The most general form of inequalities in our model is in Eq. (15) or Eq. (16). Based on these, we present detailed path of transformation of these inequalities into QUBO. Let us contract  $t$ -variables and  $y$ -variables to vectors with elements  $t_j$  and  $y_i$  (the same with constant terms  $c_i$ ). Then, from the aforementioned equations (or similar), we have:

$$t_j - t_{j'} - My_i + \xi_i = -c_i. \quad (29)$$

To replace inequalities with equalities, we use slack variables

$$0 \leq \xi_i \leq \bar{\xi}_i \text{ where } \bar{\xi}_i = -\min(t_j - t_{j'} - My_i) - c_i = -v_j + v_{j'} + d_{\max} + M_i - c_i = d_{\max} + M_i, \quad (30)$$

as  $\min(t_j) = v_j$ , and  $\max(t_j) = v_j + d_{\max}$  from Eq. (5), and we expect  $v_{j'} = v_j + c_i$ . Observe that some of the inequalities such as these of the **minimal passing time** constraints in Eq. (14) do not have order variables ( $y$  or  $z$ ), for such variables  $\bar{\xi}_i = d_{\max}$ .

To convert the constrained problem in Eq. (29) into the unconstrained one, we use the penalty method: each constraint violation is penalized by the hard constraint penalty  $p > 0$ . Such a penalty has to be sufficiently large not to be overruled by the objective. Then, the optimization problem has the form:

$$\min_{t_1, \dots, t_{j'}, \dots, \xi_1, \dots} p \sum_{(j, j', i) \in I} (t_j - t_{j'} - M_i y'_i + \xi_i + c_i)^2 + p \sum_{(i, i') \in I'} (y'_i - y'_{i'})^2 + \text{objective}. \quad (31)$$

The first sum yields inequalities (mpt, mh, d, zc constraints) and takes  $M_i = 0$  if no order variable is included. The set  $I$  contains all indices tied to these constraints, yielding  $|I| = m$  (c.f. Eq. (27)). The number of slack variables is also equal to  $m$ , as we have one slack variable per inequality. The second sum is for equates to (no) constraint and (d) constraint. Then,  $I'$  contains all indices tied to this constraint, and  $|I'| = \#_{\text{no}} + \#_d$ .

Finally (following Eq. (5) in<sup>27</sup>), we replace all  $t_j$  and  $\xi_i$  with the corresponding monomial of bits  $\sum_k d_k b_k$  where  $b_k$  are new bits variables. This transforms the quadratic unconstrained model into the quadratic unconstrained binary model. We have  $\#t$   $t$ -variables (with  $d_{\max} + 1$  distinct values) and  $m$  slack variables (with at most  $d_{\max} + \max_i \xi_i + 1$  distinct values). Referring to Eq. (27), the number of binary variables in QUBO representation can be limited by

$$\#QUBO \leq \#t \lceil \ln_2(d_{\max} + 1) \rceil + m \lceil \ln_2(d_{\max} + \max_i \xi_i + 1) \rceil + \#y + \#z. \quad (32)$$

The size of the problem (in terms of the number of QUBO variables) scales linearly with the number of zones and quadratically in the number of AGVs. The number of constraints per variable (the mean vertex degree of the graph model) is tied to the expansion of quadratic terms in Eq. (31). In Tab. 3, sizes of actual problems in terms of Ising variables (derived directly from QUBO) are presented.

For the 15 AGVs and 7 zones problem we have 696 variables (upper limit according to Eq. (12) was 945), and 1378 linear constraints (upper limit according to Eq. (28) (27) was 5513). These limits are quadratic in the number of AGVs and linear in the number of zones. We may expect the problem size to be quadratic with the number of AGVs as the number of zones is constant. If, however, the number of AGVs increases further, more zones will appear where collisions occur, and therefore, the problem size will scale worse than quadratic.

## B Details of one particular AGV problem

In this Appendix, we present a step-by-step solution of the 7 AGVs and 7 zones problem with topology presented in Fig 3. We have bi-directional lanes between zones  $s_0, s_1, s_2, s_3, s_4$  and  $s_5$  as well uni-directional lane between zones  $s_5$  and  $s_6$ . For this



$ J  /  S $	n.o. qubits (vertices)	n.o. quadratic couplings edges	edge density <sup>41</sup> $\frac{edges}{fullgraph}$	n.o. linear fields
2 / 4	122	1066	0.14	121
4 / 4	268	2644	0.07	267
6 / 7	796	11954	0.04	782
7 / 7	1204	19084	0.03	1183
12 / 7	6357	116422	0.006	6250
15 / 7	7343	134415	0.005	7219

**Table 3.** Sizes of analyzed AGV problems, in terms of Ising approach. Observe, that for the density is of the order of magnitudes lower, than the one for corresponding full graph. Concerning the largest problem, the factor is 0.005.

particular computation, the following parameters have been chosen:  $\tau^{\text{headway}} = 2$  (for all pairs of AGVs)  $\tau^{\text{zone}} = 2$  (for all AGVs), passing times (for each AGV):  $\tau^{\text{pass}}(s_0, s_1) = \tau^{\text{pass}}(s_1, s_2) = \tau^{\text{pass}}(s_3, s_4) = 6$ ,  $\tau^{\text{pass}}(s_2, s_3) = 0$ ,  $\tau^{\text{pass}}(s_4, s_5) = \tau^{\text{pass}}(s_5, s_6) = 4$ .

Then, we assume that each AGV (denoted by  $j$ ) is ready to enter its initial station (denoted by  $s_{j,0}$ ) at  $v_{in}(j, s_{j,0})$ . We also assume that AGVs have the following paths and initial conditions:

$$\begin{aligned}
& \text{AGV}_0 : \{s_0, s_1, s_2, s_3\}, v_{in}(j_0, s_0) = 0 & \text{AGV}_1 : \{s_0, s_1, s_2\}, v_{in}(j_1, s_0) = 0 \\
& \text{AGV}_2 : \{s_4, s_3, s_2, s_1\}, v_{in}(j_2, s_4) = 8 & \text{AGV}_3 : \{s_4, s_3, s_2, s_1, s_0\}, v_{in}(j_3, s_4) = 9 \\
& \text{AGV}_4 : \{s_2, s_3\} v_{in}(j_4, s_2) = 15 & \text{AGV}_5 : \{s_6, s_5, s_4, s_3\} v_{in}(j_5, s_6) = 0 \\
& \text{AGV}_6 : \{s_5, s_6\} v_{in}(j_6, s_5) = 0
\end{aligned} \tag{33}$$

In practice, the above will be done by step 2 of Algorithm in Section 3.1. In objective function in Eq. (13) for this computational example each AGV is assigned an equal weight of  $w_j = 1$ . Further, we set  $d_{\max} = 40$ .

The most important step of the Algorithm in Section 3.1 is step 5: solving the optimization problem. The CQM hybrid solver yields many solutions at a time. The best solution coincides with the optimal one also provided by CPLEX. However other solutions can also be of use for the decision support system. The solutions are presented in the form of a simplified time-space diagram (in which known points are connected with lines) in Fig. 7.

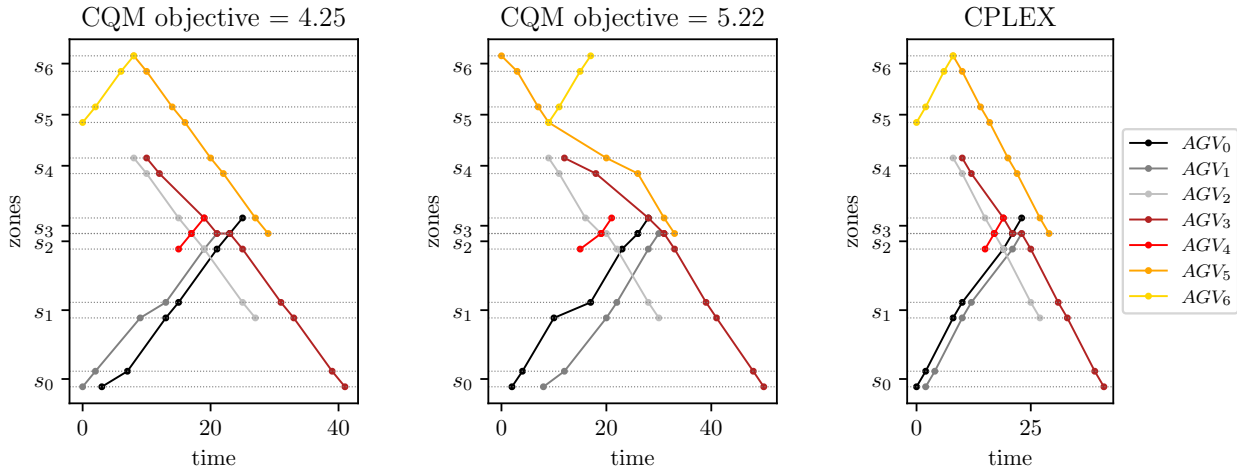


**Figure 7.** Solution in the form of a space-time diagram, two suboptimal CQM solutions and an optimal one obtained with both CQM and CPLEX. The suboptimal solutions can also be useful for the decision support system.